



# Images of the Ultra-High Energy Cosmic Rays from Point Sources

Konstantin Dolgikh<sup>a,d,\*</sup>, Alexander Korochkin<sup>b</sup>, Grigory Rubtsov<sup>a</sup>, Dmitry Semikoz<sup>c</sup>, Igor Tkachev<sup>a</sup>

<sup>a</sup>Institute for Nuclear Research of the Russian Academy of Sciences, avenue of the 60th anniversary of October, 7A, Moscow, 117312, Russia

<sup>b</sup>Université Libre de Bruxelles, CP225 Boulevard du Triomphe, Brussels, 1050, Belgium

<sup>c</sup>APC, Université Paris Cité, CNRS/IN2P3, CEA/IRFU, Observatoire de Paris, Paris, 119 75205, France

<sup>d</sup>Lomonosov Moscow State University, Faculty of Physics, Leninskie gory, 1, Moscow, 119991, Russia

Received 7 December 2023; Received in final form 25 June 2024; Accepted 20 June 2024;

Available online June 2024

## Abstract

Our latest paper (Dolgikh et al., 2023) investigates the effects of UHECR propagation in a turbulent intergalactic magnetic field in the small-angle scattering regime, specifically focusing on the non-trivial caustic-like pattern that arises with strong deviation from isotropy. In this paper, we explore the effect of the observer's position on the measurement of source flux at a given distance. We examine three types of source locations, characterized by the density of cosmic rays from a given source at the observation point, which we call magnetic knots, magnetic filaments and magnetic voids. We also investigate the energy spectrum in these different cases and present simulated images of the source as it appears on the observer's telescope after propagation in the combination of intergalactic and Galactic magnetic fields. We show that hot spots in the UHECR data can arrive due to combined distortions of the source images on the intergalactic and Galactic magnetic fields. Also the fact that flux of most nearby sources is diluted in the magnetic voids affects source population studies.

© 2024 COSPAR. Published by Elsevier Ltd All rights reserved.

**Keywords:** UHECR; IGMF; Numeric simulations

## 1. Introduction

Contrary to photons and neutrinos, Ultra-High Energy Cosmic Rays (UHECR) are charged particles and they are unavoidably deflected in the Galactic and intergalactic magnetic fields (IGMF). Expected large number of UHECR sources in the Universe together with large deflections of UHECR from source positions prevents us from doing astronomy except for the highest energies  $E > 6 \cdot 10^{19}$  eV, where the spectrum has a cutoff due to interactions with the Cosmic Microwave Background (CMB). This so-called GZK cutoff was predicted by Greisen, Zatsepin and Kuzmin in 1966 (Greisen, 1966; Zatsepin & Kuzmin, 1966). Both original papers (Greisen, 1966) and (Zatsepin & Kuzmin, 1966) provide calculations of pion photoproduction by the proton primaries while at the same time point to the effect of photodisintegration which takes place in the case of primary nuclei at nearly the same energy, see Kampert et al. (2012) for historical review.

\*Corresponding author: e-mail: [dolgikh.ka15@physics.msu.ru](mailto:dolgikh.ka15@physics.msu.ru);

Email addresses: [dolgikh.ka15@physics.msu.ru](mailto:dolgikh.ka15@physics.msu.ru) (Konstantin Dolgikh), [alexander.korochkin@ulb.be](mailto:alexander.korochkin@ulb.be) (Alexander Korochkin), [rgbeast@yandex.ru](mailto:rgbeast@yandex.ru) (Grigory Rubtsov), [dmitri.semikoz@apc.univ-paris7.fr](mailto:dmitri.semikoz@apc.univ-paris7.fr) (Dmitry Semikoz), [tkachev@ms2.inr.ac.ru](mailto:tkachev@ms2.inr.ac.ru) (Igor Tkachev)

The cutoff in the cosmic ray spectrum was observed 40 years later by the High Resolution Fly's Eye (HiRes) experiment in 2007 (Abbasi et al., 2008) and was confirmed shortly thereafter with higher exposure by the Pierre Auger Observatory (Auger) in 2008 (Abraham et al., 2008). Later in 2013 the cutoff was supported by the Telescope Array (TA) results (Abu-Zayyad et al., 2013). Recent Auger measurements show that the observed spectrum suppression may be the result of the combination of the impact of the maximum possible acceleration energy of heavy nuclei in the sources and the GZK effect (Aab et al., 2020). In certain models, see e.g. Eichmann et al. (2022), the ultra-high energy part of the cosmic ray spectrum is dominated with the local sources. In the latter case the maximum energy of acceleration determines the maximum energy of the cosmic rays. The existence of the GZK effect guarantees that UHECRs with energies  $E > 6 \cdot 10^{19}$  eV come from the local Universe with significant contribution of sources located in nearby Large Scale Structures (LSS) with a distance to our Milky Way galaxy  $R < 200$  Mpc. Since the LSS at those distances is significantly non-uniform, this gives a hope to see individual UHECR sources. Astronomy with UHECRs at the highest energies  $E > 6 \cdot 10^{19}$  eV was one of the main motivations for the construction of the Auger and TA experiments.

For cosmic ray protons deflection in the  $B_{\text{Gal}} \sim \mu\text{G}$  Galactic magnetic field is only a few degrees for  $E > 6 \cdot 10^{19}$  eV depending on the direction. At the same time even the strongest possible IGMFs with the strength of the order of  $B_{\text{IGMF}} \leq n\text{G}$  are again not efficient to disturb the UHECR proton directions from point sources. Thus one expects to see point or slightly extended sources of protons  $E > 6 \cdot 10^{19}$  eV in UHECR data. However, even with a large exposure Auger and TA have not found any signature of point sources. This observation is consistent with the statement made by Auger that most of the UHECRs with  $E > 6 \cdot 10^{19}$  eV are intermediate and heavy nuclei. In the case of heavy nuclei, the Galactic magnetic field disturbs and even washes out images of UHECR sources (Giacinti et al., 2010, 2011).

After years of observation, Auger and TA see several anomalies in the sky that look like hot spots with a radius of 10-20 degrees. These hot spots can be images of nearby point sources, disturbed both in Galactic and extragalactic magnetic fields.

Previous studies have explored the effects of intergalactic magnetic fields on the trajectories of UHECRs. One such study, Yüksel et al. (2012), investigated the Centaurus A UHECR excess and its potential connection to the local extragalactic magnetic field. This study shows that, assuming a proton composition, the strength of the extragalactic magnetic field should be at least 20 nG. This value is in conflict with existing observational constraints (Pshirkov et al., 2016; Katz et al., 2021; Jedamzik & Saveliev, 2019). In the present work we assume a high but realistic magnetic field strength.

The main goal of the present study is to show that the observed 10-20 degree radius hot spots in the UHECR data can be signals from nearby point sources, disturbed both in the Galactic and intergalactic magnetic field. In particular, we show examples of sources, which can explain the TA hot spot. We show that a caustic-like pattern arising after propagation through the intergalactic magnetic field amplifies small number of sources in filaments and knots and at the same time reduces the contribution of most of the nearby sources.

## 2. Simulation

To obtain images and spectra of the UHECR sources, we rely on numerical simulations of the UHECR propagation. Our simulation procedure generally consists of two steps. In the first step, we propagate UHECRs in the turbulent intergalactic magnetic fields, tracing their paths until they reach the edge of our galaxy. In the second step, we consider the effect of the Galactic magnetic field and construct images at the Earth's position.

For intergalactic propagation we use 3D Monte Carlo code CRbeam<sup>1</sup>(Kalashev et al., 2023) which allows to take into account UHECR deflections in magnetic fields and interactions with the CMB and the extragalactic background light (EBL). The general setup of these simulations is the same as in our previous paper Dolgikh et al. (2023). Namely we consider the source of UHECRs surrounded with the homogeneous turbulent magnetic field with a fixed strength and correlation length. The main difference is that the source emits UHECRs not isotropically, but in the form of the directional cone with a given opening angle and an axis direction (thus isotropic source is a special case with the opening angle equals  $\pi$ ). In all simulations we keep flat profile of the cone. Another important modification is that we catch particles when they hit a small spherical observer which represents our galaxy. The radius of observer was chosen to be 100, 200 or 1000 kpc, the last one for magnetic void cases. Once the particle hits the observer, we record its energy, momentum, and position on the sphere. We subsequently use this information to reconstruct the source image.

CRbeam represents turbulent magnetic field with Kolmogorov's spectrum as a sum of plain waves with random directions and phases, following the method of Giacalone & Jokipii (1999). The number density of waves is uniform in logarithmic scale by wavenumber. We fix the number of waves to be 463 with the largest eddy being 100 larger than the smallest. A smaller number of waves may lead to an unwanted effect when a wave with the longest wavelength dominates UHECR deflection. On the other hand, bigger number of waves increase calculation time. In our previous study Dolgikh et al. (2023), we carefully verified that existence of the caustic-like patterns in UHECR spacial distribution does not depend on either the method of generating the turbulent magnetic field or its spectrum. Therefore, we believe that our result are stable with respect to the technical parameters of the magnetic field generators such as number of modes and minimum scale of the turbulence. We keep the same random seed for magnetic field generation in all simulations within the paper and use OpenMP for multiprocessing acceleration.

The magnetic field strength was set to  $B = 1$  nG and the correlation length  $\lambda_c = 1$  Mpc. The magnetic field with such  $\lambda_c$  may be produced as a result of the evolution of primordial IGMF with an initially scale-invariant power spectrum, as was shown in Mchedlidze et al. (2022). In most simulations we propagate charged particles with a rigidity of  $R = 10$  EV. Since all the sources we are considering are at the distances less than 100 Mpc, and in most cases at distances of the order of 20-30 Mpc, we neglect interactions of UHECRs with the background fields.

While the distances are small enough to neglect interactions, they are large compared to the size of the observer. Given the fact that the observer's sphere has the radius of tens and hundreds kpc and charged particles have nonnegligible deflections in IGMF with  $B \propto 1$  nG the problem of aiming at the observer arises. In practice this means that most of the simulated particles will miss the observer thus increasing the amount of computational time spent in vain. This is due to both a decrease in the angular size of the observer with distance as viewed from the source and to the fact that statistically more often the observers find themselves in the regions of space where the cosmic ray flux from the source is lower than expected from standard inverse-square law (Dolgikh et al., 2023). This prompts the need of a targeting algorithm which could reduce the number of misses.

This problem was already studied earlier. For example in Jasche et al. (2020) to increase the probability of hitting the observer the initial directions of particle momentum are drawn from the von Mises–Fisher distribution with parameters adjusted as the number of detected particles increases. Here we develop a new targeting algorithm to optimize the performance.

Our algorithm is iterative, and at each subsequent step, it heavily relies on the results obtained in the previous one. The essence of the algorithm lies in the fact that if we know the initial directions that led to hits from a distance to the observer  $D_i$ , then we assume that the successful initial direction for slightly larger distance  $D_{i+1}$ , will be close to the old ones.

---

<sup>1</sup><https://github.com/okolo/mcray>

The step  $i$  of the algorithm works as follows. The distance to the observer is set to  $D_i$  and the particles are emitted in the cone with the opening angle  $\alpha_i$  and axis direction  $\theta_i, \phi_i$ . The particles are emitted uniformly within the cone and the simulation stops once the number of particles hitting the target reaches some predefined value which we set to  $N_{\text{hit}} \approx 100$ . After that the parameters of the cone are recalculated to be used in the next iteration. The new direction of the cone axis corresponds to the average initial direction of the captured particles, while the new opening angle is set to three times the maximum angle between the initial direction of the captured particles and the new cone axis. The rescaling factor of the cone opening angle and the distance increase step size (which was set to a fraction of the Larmor radius of the particle) were determined empirically and do not have strict mathematical justification. Eventually, the algorithm terminates when  $D_i$  reaches the desired distance to the source.

All the results presented in this work (see Section 3) were obtained using this algorithm, which significantly reduced computation time. The acceleration factor compared to the isotropic source can be roughly estimated as the ratio of the total solid angle to the solid angle of the final cone  $4\pi/2\pi(1 - \cos(\theta))$ . For most of our simulations, this ratio is of the order of 100.

Finally, we take into account deflections in the Galactic magnetic field and obtain images of the sources as seen by an observer at the Earth's position inside the Galaxy. We use galactic magnetic lenses provided by CRPropa3 (Alves Batista et al., 2016, 2022), which enables efficient utilization of backtracking simulations to consider galactic deflections in forward simulations of UHECRs. In particular, we adopt the lens calculated for the JF12 model of the Galactic magnetic field ('JF12full') (Alves Batista et al., 2016) with coherent, striated and turbulent components turned on (Jansson & Farrar, 2012; Jansson & Farrar, 2012). The turbulent component was assumed to have Kolmogorov spectrum with the correlation length of 60 pc and the strength that follows the JF12 turbulent field model (Jansson & Farrar, 2012).

### 3. Results

#### 3.1. Observed fluxes

In our previous paper Dolgikh et al. (2023) we have shown that in the regime of small angle scattering UHECR from point source form a caustic pattern at distance equal to tens of coherent length from the source. This pattern consist of regions with density of UHECRs larger or smaller compared to isotropic averaged. Due to the shape of these regions on sphere around source we called them magnetic knots, filaments and voids. Typical flux in knots is 10 times larger compared to average, in filaments at least 2 times larger and in magnetic voids at least two times smaller. By average, we mean the expected flux from the source, assuming that it follows the inverse-square law.

We studied propagation of UHECR protons with energies  $E > 10^{19}$  eV in the turbulent intergalactic magnetic field with strength  $B = 1$  nG and coherent length  $\lambda_c = 1$  Mpc. For such parameters of magnetic field non-trivial UHECR pattern exist at all distances in nearby LSS up to 100 Mpc, from which most of UHECR at highest energies arrive in the Earth detectors.

First, we examine the properties of the observed signal as a function of UHECR energy and a distance to the source. In Fig. 1 we show probability that at a given distance from the source UHECR flux differs from an average one in 2 or 10 times. One can see, that most probably the flux from the given source will be lower compared to the average one. For 10 % of sources it is at least two times higher while in up to 75% of cases it is 2 times smaller. Only in a few percent of cases (located in the magnetic knots relative to the observer) the flux can be enhanced 10 times and more  $F/F_{\text{av}} > 10$ . On the other hand in up to 55 % of the cases the flux can be reduced in 10 times  $F/F_{\text{av}} < 10$  in the magnetic voids. This means that for most of the sources the UHECR flux will stay same or will be reduced, while only for a small fraction of sources it will be significantly increased, giving the possibility to

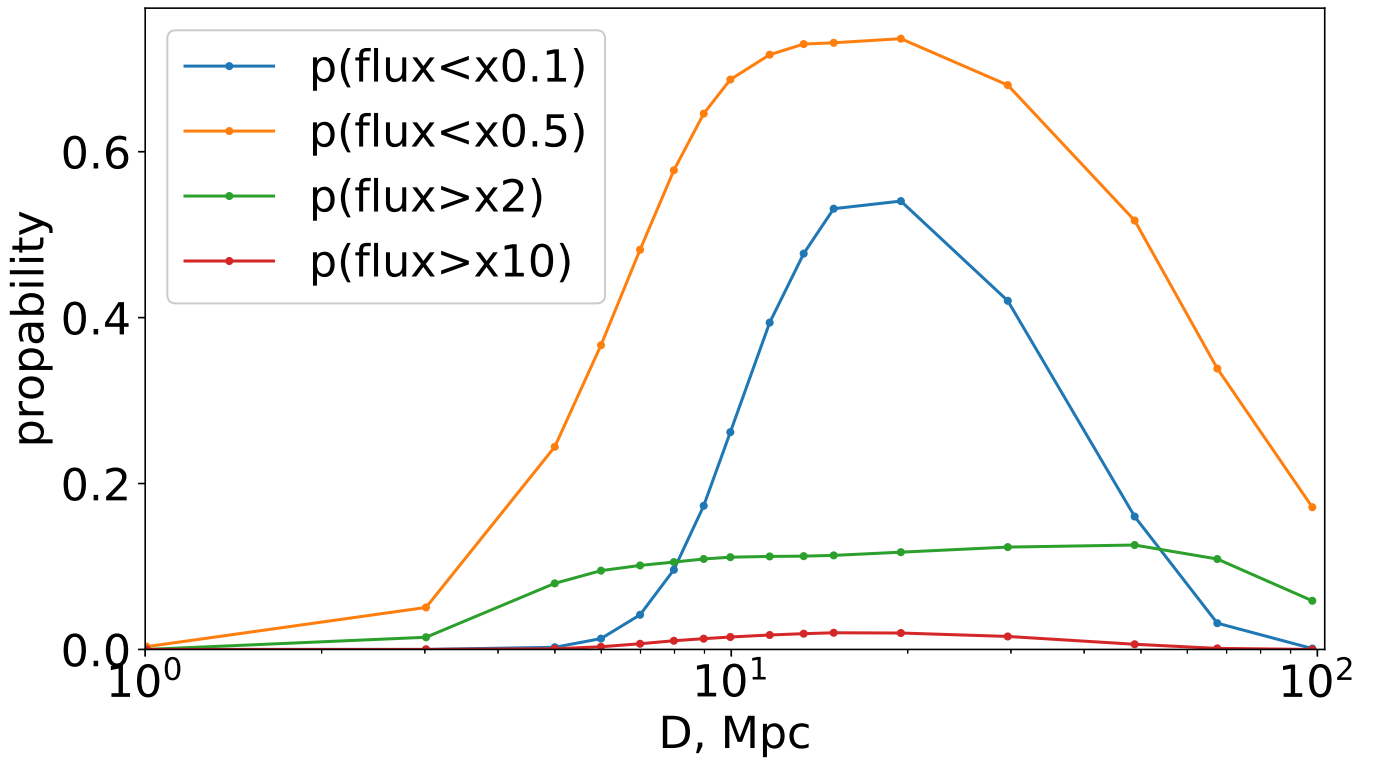


Fig. 1. Probability of observer to be located in the region with flux higher or smaller compared to an average one as function of the distance to the source for the particles with the rigidity of  $E = 10$  EV.

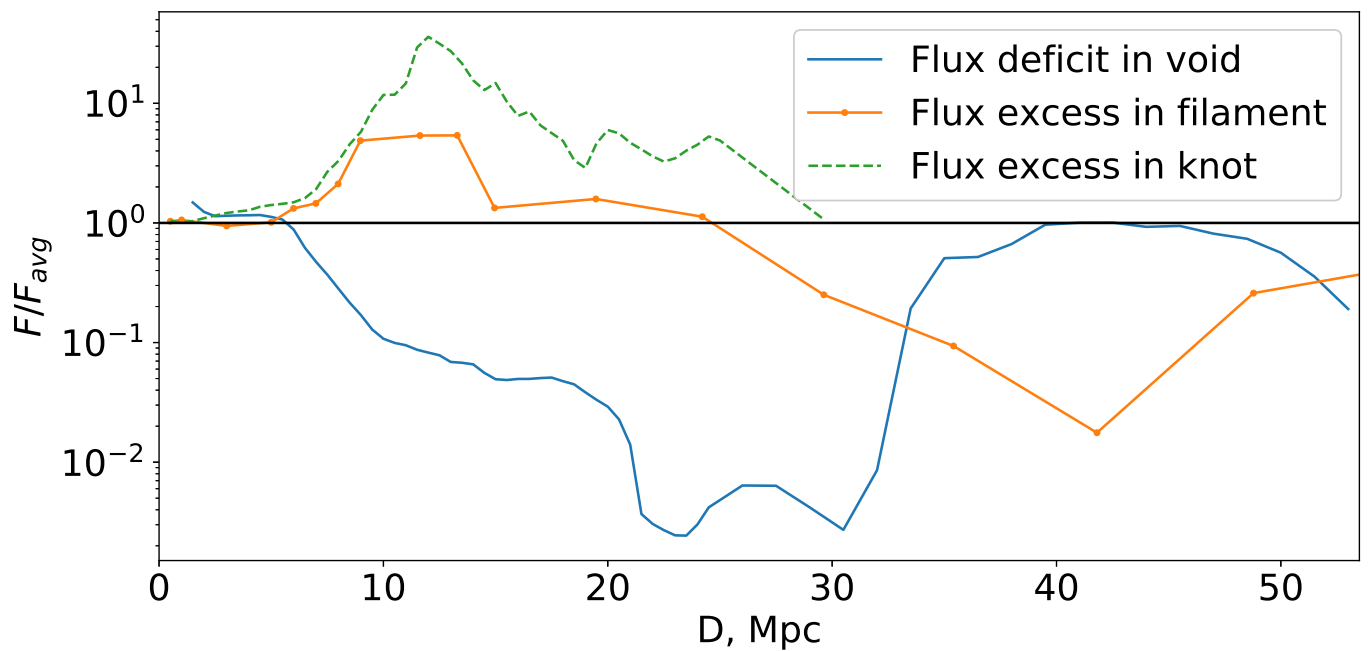


Fig. 2. Example of the relative flux excess and deficit as function of the distance to the source for the particles with the rigidity of  $E = 10$  EV. For this figure we define magnetic void, filament and knot at the distance of 10 Mpc.

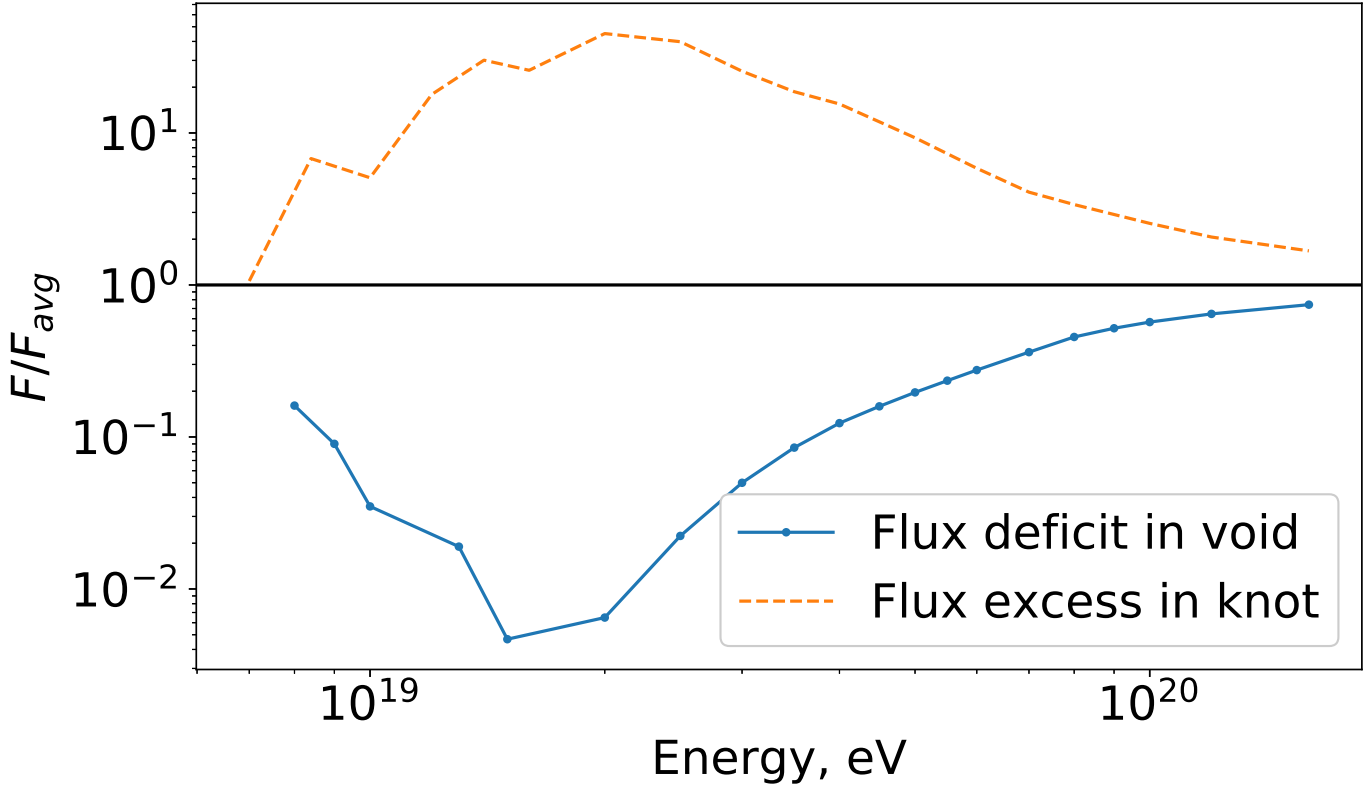


Fig. 3. Proton energy spectrum of the source seen by an observer located in the knot at the distance  $D = 20$  Mpc and in the void at  $D = 30$  Mpc. Each spectral bin is normalized to the average flux at the same energy.

observe a 'hot spot' in the UHECR spectrum. The average flux through the sphere remains the same at all distances. Particles do not interact when propagating through a magnetic field.

In Fig. 2 we show an example of  $E = 10$  EV particle fluxes relative to average one in the directions to magnetic knot, void and filament as a function of the distance from the source. For this figure the magnetic knot, void and filament are defined at the distance of 10 Mpc, see Fig. 6 in Dolgikh et al. (2023). The black solid line marks an average flux  $F = F_{av}$ . One can see that in example of Fig. 2 filament at knot have maximal flux at 12 Mpc from source and disappeared at 25-30 Mpc distance. Moreover, filament transforms into void between 30 Mpc and 50 Mpc from source.

Finally we constructed the energy spectrum of the source for an observer located in the knot and in the void, see Fig. 3. One can see that the observed flux deviates significantly from the average one at the energies around 10-30 EeV. These deviations disappear both at low and high energies. At the highest energies  $\sim 100$  EeV the deflections become too small to produce strong enough flux variations. On the other hand at low energy end of the spectrum UHECR propagation becomes diffusive which is also washing out the filamentary pattern.

### 3.2. Source images

Although the observer is quite small, its non-zero size can cause distortion of the source image. The effect is more pronounced for the sources located closer to the observer. The particles that hit the opposite edges of the observer, will have a slightly different arrival direction as seen from the center of the sphere, which is not related to the magnetic field. We take this effect into account and compensate for it in order to exclude it from the observation picture. To do this, a small correction is added to the arrival direction of the particles that hit the observer:  $\vec{p}_{end} \rightarrow \vec{p}_{end} - \frac{\vec{r}_{end}}{|\vec{r}_{end} - \vec{r}_{source}|}$ , where  $\vec{r}_{end}$  is final coordinates of the particle (observer will be in

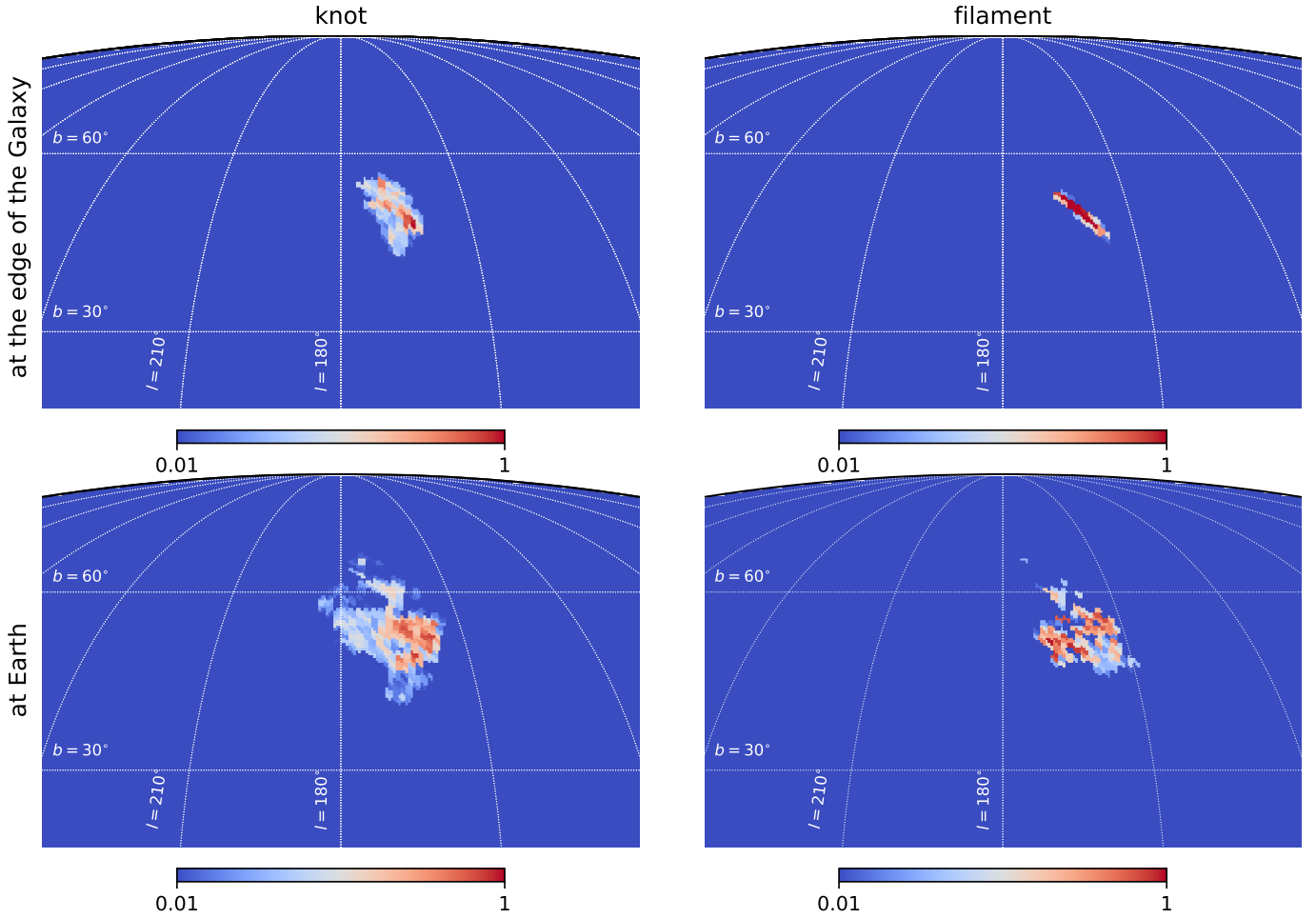


Fig. 4. Source images seen by the observer located at knot and filament calculated at the edge of the Galaxy and after propagation through the GMF. Color encodes the number of hits to a given pixel. In both cases the intrinsic source luminosity is adjusted so that total number of events from the source observed at Earth matches with the cumulative number of TA events falling inside the hot spot circle of  $25^\circ$  (44 events for the 15-year TA SD data (Kim et al., 2023)). The blue color corresponds to the background level which is shown as uniform for clarity.

$(0,0,0)$  coordinates),  $\vec{r}_{source}$  is coordinates of the source.

We have studied two cases of observer location in Fig.4: observer in a filament and observer in knot. Relative to the observer, it looks like two different environments of the extragalactic magnetic field. We didn't consider the most likely case of the magnetic void (it is about  $\sim 70\%$ , see Fig.1) as in this case the flux is extremely small and hard for detection. The knot case produces a bright smudged spot but this case is the most unlikely. Thus, if we have many sources of UHECR around us at a distance of tens Mpc, we see only a few of them. With respect to most sources, we will be in the voids. Sources at greater distances (more 100 Mpc) give an isotropic contribution, which decreases with distance and creates a uniform background.

On the top right panels of Fig.4 one can see the images of the sources at the edge of our Galaxy, i.e. before propagation through the Galactic magnetic field. When the observer is located in a magnetic filament (upper right panel) the image is very stretched. This shape of the image is not accidental and is a distinctive feature of the observer's position. The direction along which the image is stretched is always perpendicular to the magnetic filament which is the result of particle focusing. In order to have the flux enhancement in a filament, the magnetic field should bend UHECR trajectories along a direction perpendicular to the direction of the filament itself. Therefore, for an observer in the filament, particles will come from directions perpendicular to the filament. To

the contrary, in the case of the observer in the magnetic knot, the image is more symmetric.

After passing the Galactic magnetic field, a smeared spots could be formed as in the bottom panels of Fig.4. To be more specific, the positions of the sources in the sky were chosen in a way to correspond to the TA hotspot direction before GMF lensing. The quantitative prediction will certainly depend on the specific GMF model used, but the overall picture will stay the same. The uncertainty of the UHECR deflections in the GMF was recently analysed in Unger & Farrar (2023) (in particular, see Fig. 18 of Unger & Farrar (2023)).

In order to analyze the size of the spot we have repeated the analysis performed by Telescope Array collaboration for the search of the hotspot (Abbasi et al., 2014) with the event set randomly generated using the density seen by the observer located at knot and filament as shown in the bottom panels of Fig.4. We have found that the maximum Li-Ma statistics in both cases corresponds to the 15 degrees oversampling radius, which is of the same order of magnitude as the sizes of known hotspots in the UHECR data. The hotspot observation is consistent with the discussed scenario. At the same time, under the latter scenario, some of the sources fall into the void, which requires an increased overall source density.

We performed an analysis for the particles of the rigidity 10-20 EV. Since UHECRs at the highest energies can be dominated by intermediate nuclei according to the Auger data, propagation of particles of those rigidities would correspond to propagation of nuclei with  $Z$  times larger energies in the same magnetic fields. In particular UHECRs with  $E > 57$  EeV would correspond to CNO nuclei. As was shown for example in Neronov et al. (2023), CNO nuclei of required energies can reach us from up to 70 Mpc distance.

#### 4. Conclusions

In this paper we studied the influence of the intergalactic and Galactic magnetic fields on the images of nearby sources in the UHECR data. In particular we studied the possibility of explaining the hot spots in UHECR data by the contribution of nearby sources. In our previous paper Dolgikh et al. (2023) we have shown that the effects of UHECR propagation in a turbulent intergalactic magnetic field in the small-angle scattering regime produce a non-trivial caustic-like pattern in the spatial density of cosmic rays, with magnetic knots, filaments and voids in the density profile at a given distance from the source. Here we studied the dependence of the density profile from the distance from the source and from energy for fixed properties of the magnetic field with a strength 1 nG and a coherence length of 1 Mpc. We found that for a large range of distances and energies of UHECR, the caustic-like pattern stays similar in the sky. This means that for a given position of the Milky Way galaxy in this pattern we get (de-)amplification of original flux of the source.

Final source images after propagation in the Galactic magnetic field are shown in Fig. 4. One can see that both magnetic knot and filament structures can provide final hot spots in the UHECR image, while location in the magnetic void significantly reduce the contribution of a given source to the observed UHECR flux.

For a given class of UHECR sources we expect that most of the nearby sources are located in the magnetic voids and we see only few of sources, which are located in the filaments. With a small probability one can see even brighter amplification of the sources's flux in the knot.

Thus, in this work we show how hot spots in UHECR data can form. In Fig.4 we have shown examples of the source images in the direction of the TA hot spot. We show that after propagation in the Galactic and intergalactic magnetic fields the source image can look like the one observed in the UHECR data. We performed an analysis for 10 EV particles, which would correspond to CNO



nuclei for energies of the hot spot in the TA and Auger data  $E > 57$  EeV. Source location at several tens of Mpc is still possible for CNO nuclei of those energies.

**Acknowledgements.** Modeling of propagation of high-energy radiation in the Universe has been supported by the Russian Science Foundation grant 22-12-00253 (K.D. and G.R.). The work of K.D. has been supported by the fellowship of Basis Foundation (grant No. 22-1-5-92-1). The work of A.K. has been supported by the IISN project No. 4.4501.18. Some of the results in this paper have been derived using the healpy and HEALPix<sup>2</sup>(Górski et al., 2005) packages.

## References

- Aab, A. et al. (Pierre Auger) (2020). Features of the Energy Spectrum of Cosmic Rays above  $2.5 \times 10^{18}$  eV Using the Pierre Auger Observatory. *Phys. Rev. Lett.*, 125(12), 121106. doi:10.1103/PhysRevLett.125.121106. arXiv:2008.06488.
- Abbasi, R. U. et al. (HiRes) (2008). First observation of the Greisen-Zatsepin-Kuzmin suppression. *Phys. Rev. Lett.*, 100, 101101. doi:10.1103/PhysRevLett.100.101101. arXiv:astro-ph/0703099.
- Abbasi, R. U. et al. (Telescope Array) (2014). Indications of Intermediate-Scale Anisotropy of Cosmic Rays with Energy Greater Than 57 EeV in the Northern Sky Measured with the Surface Detector of the Telescope Array Experiment. *Astrophys. J. Lett.*, 790, L21. doi:10.1088/2041-8205/790/2/L21. arXiv:1404.5890.
- Abraham, J. et al. (Pierre Auger) (2008). Observation of the suppression of the flux of cosmic rays above  $4 \times 10^{19}$  eV. *Phys. Rev. Lett.*, 101, 061101. doi:10.1103/PhysRevLett.101.061101. arXiv:0806.4302.
- Abu-Zayyad, T. et al. (Telescope Array) (2013). The Cosmic Ray Energy Spectrum Observed with the Surface Detector of the Telescope Array Experiment. *Astrophys. J. Lett.*, 768, L1. doi:10.1088/2041-8205/768/1/L1. arXiv:1205.5067.
- Alves Batista, R., Dundovic, A., Erdmann, M. et al. (2016). CRPropa 3 - a Public Astrophysical Simulation Framework for Propagating Extraterrestrial Ultra-High Energy Particles. *JCAP*, 05, 038. doi:10.1088/1475-7516/2016/05/038. arXiv:1603.07142.
- Alves Batista, R. et al. (2022). CRPropa 3.2 — an advanced framework for high-energy particle propagation in extragalactic and galactic spaces. *JCAP*, 09, 035. doi:10.1088/1475-7516/2022/09/035. arXiv:2208.00107.
- Dolgikh, K., Korochkin, A., Rubtsov, G. et al. (2023). Caustic-Like Structures in UHECR Flux after Propagation in Turbulent Intergalactic Magnetic Fields. *J. Exp. Theor. Phys.*, 136(6), 704–710. doi:10.1134/S1063776123060031. arXiv:2212.01494.
- Eichmann, B., Kachelrieß, M., & Oikonomou, F. (2022). Explaining the UHECR spectrum, composition and large-scale anisotropies with radio galaxies. *JCAP*, 07(07), 006. doi:10.1088/1475-7516/2022/07/006. arXiv:2202.11942.
- Giacalone, J., & Jokipii, J. R. (1999). The transport of cosmic rays across a turbulent magnetic field. *Astrophys. J.*, 520(1), 204. URL: <https://dx.doi.org/10.1086/307452>. doi:10.1086/307452.
- Giacinti, G., Kachelrieß, M., Semikoz, D. V. et al. (2010). Ultrahigh Energy Nuclei in the Galactic Magnetic Field. *JCAP*, 08, 036. doi:10.1088/1475-7516/2010/08/036. arXiv:1006.5416.
- Giacinti, G., Kachelrieß, M., Semikoz, D. V. et al. (2011). Ultrahigh Energy Nuclei in the Turbulent Galactic Magnetic Field. *Astropart. Phys.*, 35, 192–200. doi:10.1016/j.astropartphys.2011.07.006. arXiv:1104.1141.
- Górski, K. M., Hivon, E., Banday, A. J. et al. (2005). HEALPix: A Framework for High-Resolution Discretization and Fast Analysis of Data Distributed on the Sphere. *Astrophys. J.*, 622, 759–771. doi:10.1086/427976. arXiv:astro-ph/0409513.
- Greisen, K. (1966). End to the cosmic ray spectrum? *Phys. Rev. Lett.*, 16, 748–750. doi:10.1103/PhysRevLett.16.748.
- Jansson, R., & Farrar, G. R. (2012). A New Model of the Galactic Magnetic Field. *Astrophys. J.*, 757(1), 14. doi:10.1088/0004-637X/757/1/14. arXiv:1204.3662.
- Jansson, R., & Farrar, G. R. (2012). The Galactic Magnetic Field. *Astrophys. J. Lett.*, 761, L11. doi:10.1088/2041-8205/761/1/L11. arXiv:1210.7820.
- Jasche, J., van Vliet, A., & Rachen, J. P. (2020). Targeting Earth: CRPropa learns to aim. *PoS, ICRC2019*, 447. doi:10.22323/1.358.0447. arXiv:1911.05048.
- Jedamzik, K., & Saveliev, A. (2019). Stringent Limit on Primordial Magnetic Fields from the Cosmic Microwave Background Radiation. *Phys. Rev. Lett.*, 123(2), 021301. doi:10.1103/PhysRevLett.123.021301. arXiv:1804.06115.
- Kalashov, O., Korochkin, A., Neronov, A. et al. (2023). Modeling the propagation of very-high-energy  $\gamma$ -rays with the CRbeam code: Comparison with CRPropa and ELMAG codes. *Astron. Astrophys.*, 675, A132. doi:10.1051/0004-6361/202243364. arXiv:2201.03996.
- Kampert, K.-H., Watson, A. A., & Watson, A. A. (2012). Extensive Air Showers and Ultra High-Energy Cosmic Rays: A Historical Review. *Eur. Phys. J. H*, 37, 359–412. doi:10.1140/epjh/e2012-30013-x. arXiv:1207.4827.
- Katz, H. et al. (2021). Introducing SPHINX-MHD: the impact of primordial magnetic fields on the first galaxies, reionization, and the global 21-cm signal. *Mon. Not. Roy. Astron. Soc.*, 507(1), 1254–1282. doi:10.1093/mnras/stab2148. arXiv:2101.11624.
- Kim, J., Ivanov, D., Kawata, K. et al. (Telescope Array) (2023). Anisotropies in the arrival direction distribution of ultra-high energy cosmic rays measured by the Telescope Array surface detector. *PoS, ICRC2023*, 244. doi:10.22323/1.444.0244.
- Mtchedlidze, S., Domínguez-Fernández, P., Du, X. et al. (2022). Evolution of Primordial Magnetic Fields during Large-scale Structure Formation. *Astrophys. J.*, 929(2), 127. doi:10.3847/1538-4357/ac5960. arXiv:2109.13520.
- Neronov, A., Semikoz, D., & Kalashov, O. (2023). Limit on the intergalactic magnetic field from the ultrahigh-energy cosmic ray hotspot in the Perseus-Pisces region. *Phys. Rev. D*, 108(10), 103008. doi:10.1103/PhysRevD.108.103008. arXiv:2112.08202.
- Pshirkov, M. S., Tinyakov, P. G., & Urban, F. R. (2016). New limits on extragalactic magnetic fields from rotation measures. *Phys. Rev. Lett.*, 116(19), 191302. doi:10.1103/PhysRevLett.116.191302. arXiv:1504.06546.
- Unger, M., & Farrar, G. R. (2023). The Coherent Magnetic Field of the Milky Way. *Accepted for publication in Astrophys. J.*, . arXiv:2311.12120.
- Yüksel, H., Stanev, T., Kistler, M. D. et al. (2012). THE CENTAURUS A ULTRAHIGH-ENERGY COSMIC-RAY EXCESS AND THE LOCAL EXTRAGALACTIC MAGNETIC FIELD. *Astrophys. J.*, 758(1), 16. URL: <https://doi.org/10.1088/0004-637x/758/1/16>. doi:10.1088/0004-637x/758/1/16.
- Zatsepin, G. T., & Kuzmin, V. A. (1966). Upper limit of the spectrum of cosmic rays. *JETP Lett.*, 4, 78–80. [Pisma Zh. Eksp. Teor. Fiz.4,114(1966)].

<sup>2</sup><http://healpix.sf.net>